Quantitative Analyses of Aluminium Alloy Corrosion Pit Surface Morphology Based on Box-counting Fractal Dimension

Guangyao Yan [1], Zhiguo Liu [1], Tao Liu [1], Xudong Li [1], Yuhui Ma [2]

[1]Aviation Mechanics Department, Qingdao Branch of Naval Aeronautical University, Qingdao 266041, China
[2]The Chinese People's Liberation Army 92635 Troop, China.

Abstract. All manuscripts must be in English, also the table and figure texts, otherwise we cannot publish your paper. Please keep a second copy of your manuscript in your office. When receiving the paper, we assume that the corresponding authors grant us the copyright to use the paper for the book or journal in question. Should authors use tables or figures from other Publications, they must ask the corresponding publishers to grant them the right to publish this material in their paper.

Keywords: Accelerated corrosion test; Pit surface outline; Box-counting fractal dimension; quantitative analysis.

1. Introduction

Based on high specific strength and good processing performance, aluminum alloy is widely used in aviation industry. Aviation aluminum alloy is more prone to corrosion suffering external natural environment. In the initial corrosion stage, pit corrosion is the main corrosion form which will reduce the mechanical properties and pose a threat to flight safety. From now on, a great deal of researches has been made on corrosion pit morphology in all fields. For instance, literatures [1-3] qualitatively analyzed the features of pit morphology and studied how one corrosion characteristic factor impacted on structural component fatigue properties, establishing the corresponding empirical correlations. Literatures [4-8] quantitatively analyzed the characteristics of multiple corrosion pit morphology by using image digital processing method. Some scholars took single corrosion pit as the research object, such as Zhang [9] defined the parameter AB to expediently classify pit shapes. Xing [10] defined the parameter B and C/A to analyze the two corrosion damage indexes influences on fatigue life. Some scholars studied corrosion surface morphology by using fractal theory, for example literature [11] quantitatively analyzed the surface roughness fractal dimension and found the relationship between fractal dimension values and corrosion levels.

However, there were few studies on corrosion pit surface outline fractal features in the accelerated corrosion test environment up to now. A certain aircraft serves at an airport in Hainan, and above 90% service time is spent on parking. This airport belongs to typical coastal environment, so that aircraft aluminum alloy structural components are easy to be corroded. By collecting and sifting the environment factors of the airport, and using surface current density as converting coefficient, this paper designed the aluminum alloy accelerated corrosion test spectrum equivalently according to

spectrum conducting process [12-15]. The corresponding accelerated corrosion test was carried out consequently. Every equivalent corrosion year, typical corrosion pit morphology was analyzed statistically and surface and inner pit outlines fractal features were extracted, thereupon the evolution rules of corrosion morphology was studied quantitatively. This paper enriched quantitative research means of aviation aluminum alloy corrosion morphology and provided data support on corrosion pit finite element modeling.

1.1. The box-counting fractal dimension

The box-counting fractal dimension has been widely used because of its intuitive definition. The definition emerged from the 1930s, and it got many alternative names, such as, the entropy dimension, the logarithmic dimension and the information dimension etc.

Suppose F is an upper bounded nonvoid subset of Rn, and $N_\delta(\mathrm{F})$ represents the minimum number of a set covering set F, of which the maximum diameter is δ. Thus, the definitions of the lower and upper box-counting fractal dimension respectively are:

$$\underline{\dim}_B \mathrm{F} = \underline{\lim}_{\delta \to 0} \frac{\log N_\delta(\mathrm{F})}{-\log \delta} \tag{1}$$

$$\overline{\dim}_B \mathrm{F} = \overline{\lim}_{\delta \to 0} \frac{\log N_\delta(\mathrm{F})}{-\log \delta} \tag{2}$$

If equation (1) is equal to equation (2), then it is regarded as the box-counting fractal dimension of set F denoted as:

$$\dim_B \mathrm{F} = \lim_{\delta \to 0} \frac{\log N_\delta(\mathrm{F})}{-\log \delta} \tag{3}$$

In actual engineering problems, fractal dimension is always defined as difference box-counting fractal dimension denoted as:

$$\dim_{\mathrm{DB}} \mathrm{F} = \frac{\Delta(\log N_\delta(\mathrm{F}))}{-\Delta(\log \delta)} \tag{4}$$

For the two-dimensional box-counting fractal dimension method, generally, five element cells are employed to define scale δ to finally compute $N_\delta(\mathrm{F})$, and they are:

(1) Closed ball containing F which radius is δ, $N_\delta(\mathrm{F})$ is the lower limit number;

(2) Square containing F which edge length is δ, $N_\delta(\mathrm{F})$ is the lower limit number;

(3) δ net squares intersecting with F, $N_\delta(\mathrm{F})$ is the number;

(4) Set containing F which maximum diameter is δ, $N_\delta(\mathrm{F})$ is the lower limit number;

(5) Closed ball which center is in set F and which radius is δ, $N_\delta(\mathrm{F})$ is the upper limit number of the mutually disjoint sets.

Consider $\delta-$ net cubes in Rn, namely cubes in form of $[m_1\delta,(m_1+1)\delta]\times\cdots\times[m_n\delta,(m_n+1)\delta]$ of which $m_1,\cdots,m_n$ are integers, so 'cube' R_1 means interval and 'cube' R_2 means square. Suppose $N_\delta'(\mathrm{F})$ is the number of intersecting between $\delta-$ net cubes and set F. Obviously, it represents cubes

with the number of $N_{\delta}^{'}(\mathrm{F})$ of which diameters are $\delta\sqrt{n}$, on the other hand, every set which maximum diameter is δ is covered by $\delta-$net cubes with the number of 3^n, so there is:

$$N_{\delta\sqrt{n}}(\mathrm{F}) \le N_{\delta}\,'(\mathrm{F}) \le 3^n N_{\delta}(\mathrm{F}) \tag{5}$$

Consider left side of the above, if $\delta\sqrt{n}<1$, then:

$$\frac{\log N_{\delta\sqrt{n}}(\mathrm{F})}{-\log(\delta\sqrt{n})} \le \frac{\log N_{\delta}\,'(\mathrm{F})}{-\log\sqrt{n}-\log\delta} \tag{6}$$

Make $\delta\to 0$, the lower limit and upper limit are:

$$\underline{\dim}_B \mathrm{F} \le \underline{\lim}_{\delta\to 0}\frac{\log N_{\delta}\,'(\mathrm{F})}{-\log\delta} \tag{7}$$

$$\overline{\dim}_B \mathrm{F} \le \overline{\lim}_{\delta\to 0}\frac{\log N_{\delta}\,'(\mathrm{F})}{-\log\delta} \tag{8}$$

Consider right side of inequation (5), make $\delta\to 0$, then the lower limit and upper limit are:

$$\underline{\lim}_{\delta\to 0}\frac{\log N_{\delta}\,'(\mathrm{F})}{-\log\delta} \le \underline{\dim}_B \mathrm{F} \tag{9}$$

$$\overline{\lim}_{\delta\to 0}\frac{\log N_{\delta}\,'(\mathrm{F})}{-\log\delta} \le \overline{\dim}_B \mathrm{F} \tag{10}$$

In order to get the box-counting fractal dimension, $N_{\delta}\,'(\mathrm{F})$ is regarded as $N_{\delta}(\mathrm{F})$. While computing the box-counting fractal dimension of a two-dimensional set F, a square with edge length δ, known as 'box', could be made, then the irregular degree of the set will be gained while calculating different scales of δ.dimension values reflect the irregularity of a set while δ approaches zero.

2. Accelerated corrosion test

The aluminum alloy LD2CS test piece has a dog-bone shape. The figure of piece dimension and object is shown as figure 1.

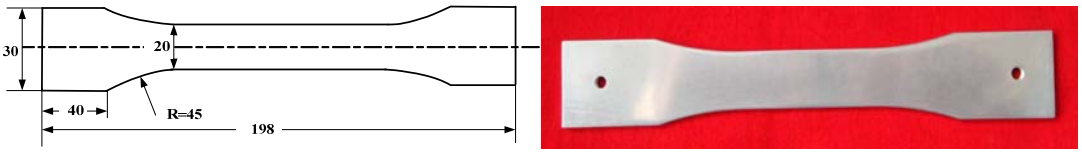

(a) test piece dimension (unit: mm, thickness: t=3mm) (b) test piece object

Fig 1. Aluminum alloy LD2CS test piece

Based on environment characteristics of the airport in Hainan, corresponding environment data were collected and sifted. According to spectrum conducting process, the environment spectrum was established, then the test surface current density is regarded as conversion coefficient to acquire the airport accelerated corrosion test spectrum, the detailed parameters are shown in figure 2.

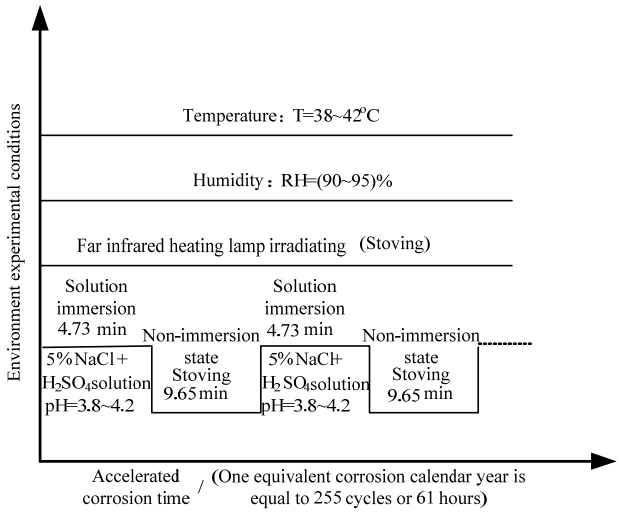

Fig 2. Accelerate corrosion spectrum of aluminum alloy LD2CS

As shown in figure 2, aluminum alloy LD2CS accelerated corroded 61hours accounts to a year of corrosion damage in the airport environment. According to parameters in the spectrum and accelerated corrosion test requirements, test pieces were put into a ZJF-45G dry-wet cyclic immersion test chamber and the experiment was conducted up to 11 equivalent years. Every equivalent year, the test pieces were taken out to do observations and statistical analyses employing the KH-7700 optical morphology detection microscope.

3. Test results and discussion

3.1. Analyses of typical corrosion pit surface outline fractal dimension

From the third equivalent calendar year, typical corrosion pits were observed and a red marker was used to mark the pits. In this paper, typical corrosion pits surface photos were preprocessed and then the two-dimensional box-counting fractal dimension values were calculated using the program written in MATLAB 7.0. Detailed procedure was described below.

(1) Corrosion pits surface morphology was photographed using the KH-7700 optical microscope, figure 3 shows the No.1 typical corrosion pit surface morphology after accelerated corroding 3, 5,7 and 9 equivalent years.

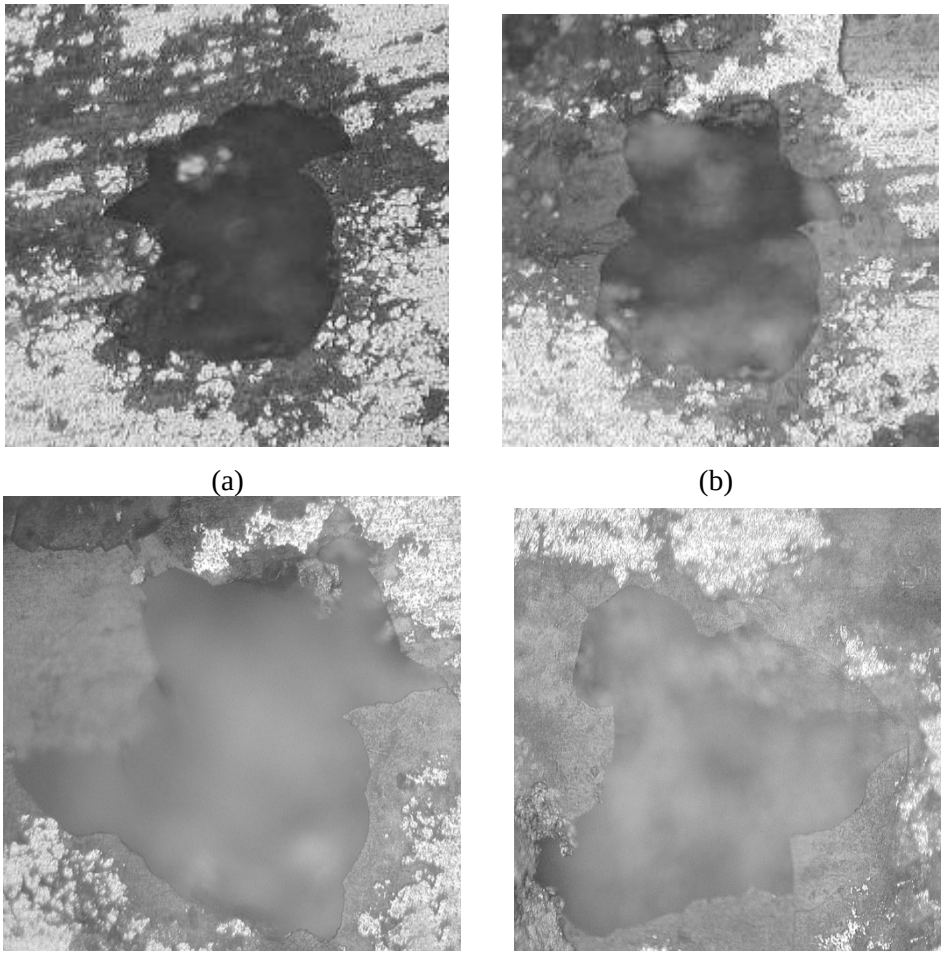

(a) (b)

(c) (d)

(a) The third year (b) The fifth year (c) The seventh year (d) The ninth year

Fig 3. No.1 typical corrosion pit surface morphology

(2) the corrosion pits surface morphology photos were contoured and outlines of the pits were gained respectively, as shown in figure 4. It was difficult to estimate which outline was more complicated than others, therefore, corrosion pits outline fractal characteristics needed to be extracted.

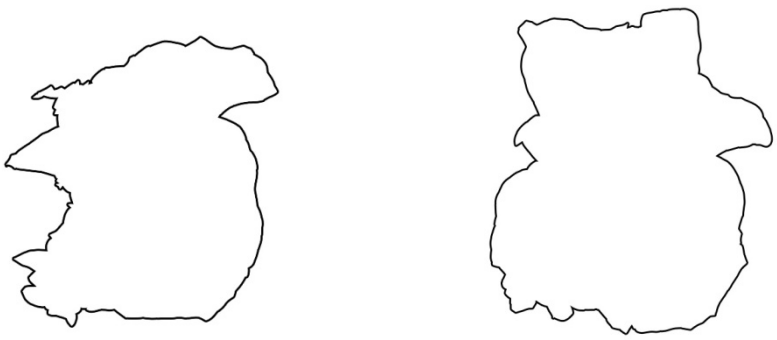

(a) (b)

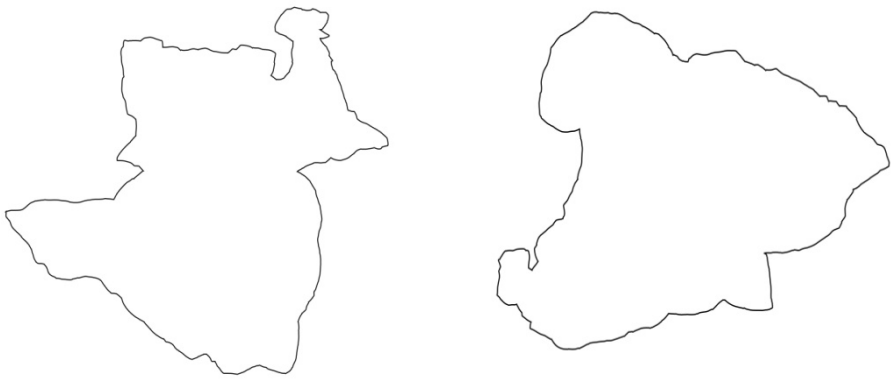

(c) (d)

(a) The third year (b) The fifth year (c) The seventh year (d) The ninth year

Fig 4. No.1 typical corrosion pit surface outlines

(3) Finite difference box-counting fractal dimension program was written in MATLAB to calculate pit surface outlines fractal dimension values after image preprocessing. Binarization method was used to process outline images and the pixel threshold was set as 80 to generate grayscale images. Corresponding number of the δ- net cubes, $N_\delta(F)$, was obtained by changing the scale δ (δ=1,2, 4,…,210). $\dim_{DB} F$ was calculated at different scales, as shown in figure 5.

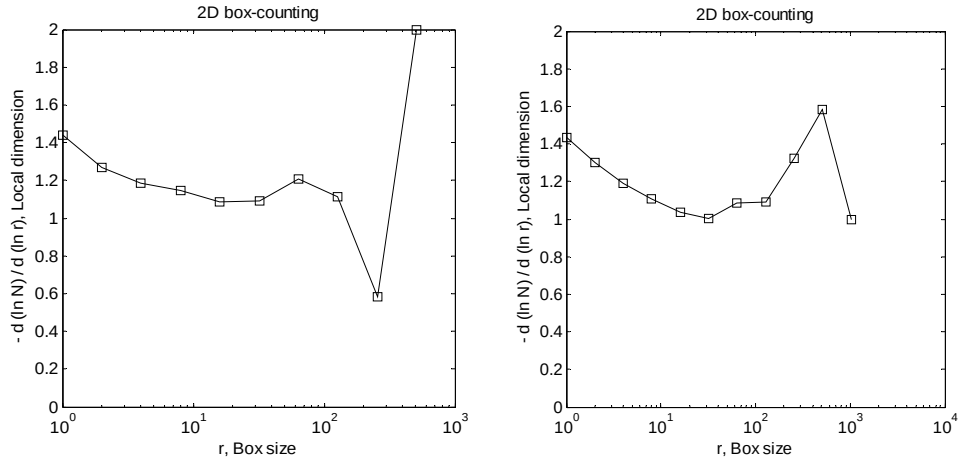

(a) The third equivalent year (b) The seventh equivalent year

Fig 5. No.1 corrosion pit surface outlines fractal dimension calculation

As shown in figure 5, generally, pit outlines fractal dimension standard deviations were larger when the scale was small or large, after considerable research, fractal dimension data were gathered statistically while δ was in the interval from 2^3 to 2^7, and the standard deviation threshold was 0.200. Three typical pit outline box-counting fractal dimension values were analyzed statistically and listed in table 1.

Table 1. Statistic data of typical corrosion pits surface outline fractal dimension

Equivalent corrosion year/a	Pit No.1		Pit No.2		Pit No.3	
	Mean value	Standard Deviation	Mean value	Standard Deviation	Mean value	Standard Deviation
3	1.118	0.103	1.210	0.261	1.101	0.059
4	1.153	0.071	1.214	0.194	——	——
5	1.156	0.041	——	——	1.092	0.065
6	1.143	0.076	1.294	0.120	——	——
7	1.135	0.053	1.180	0.072	1.143	0.091
8	1.132	0.067	1.171	0.081	1.096	0.090
9	1.084	0.073	——	——	1.087	0.098
10	——	——	1.125	0.076	1.105	0.043
11	——	——	1.077	0.064	——	——

The fractal dimension mean values of different equivalent corrosion years could quantificationally evaluated the evolvement rule of corrosion pit surface outline's complexity. Fractal dimension values of corrosion pit outlines reached the maximum in the middle of the corrosion period (from the fifth to the seventh equivalent year), relatively, the values were smaller in the earlier (from the third to the fifth equivalent year) and later period (from the seventh to the eleventh equivalent year). It demonstrated that pit surface outlines experienced a gradual process from simple to complex and then to simple, and it was found that corrosion pits surface outlines had a tendency to be smooth and long oval.

3.2. Analyses of stepped appearance fractal dimension

During the later period, stepped appearances were discovered in corrosion pits depending on variable focal length observation by QUESTAR KH-7700 optical microscope. In general, during the eighth to the eleventh accelerated corrosion years, there were 3 to 4 stepped inner corrosion pits in one surface pit, as shown in figure 6. With the method of box-counting fractal dimension figuring out that the inner pit fractal dimension value was calculated and the surface pit was supposed to be the first step pit, the deeper the pit was, the greater the step number would be. Table 2 shows the values of stepped pit fractal dimension. It demonstrated that the deeper the step pit was, the more complicated the pit outline would be.

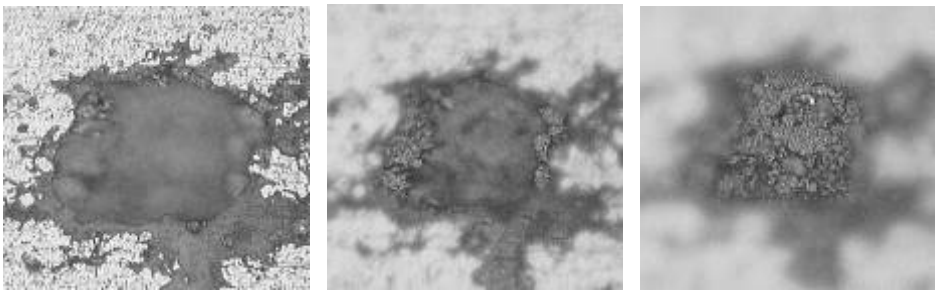

(a) The first step pit (b) The second step pit (c) The third step pit

Fig 6. Different steps of a typical corrosion pit

Table 2. Statistic data of typical pit surface profile fractal dimension in different grades

The step number of a corrosion pit	Pit No.1		Pit No.2		Pit No.3	
	Mean value	Standard Deviation	Mean value	Standard Deviation	Mean value	Standard Deviation
1	1.189	0.077	1.115	0.039	1.126	0.081
2	1.205	0.217	1.165	0.037	1.223	0.082
3	1.103	0.062	1.129	0.075	1.187	0.180
4			1.241	0.081	1.197	0.230

4. Conclusion

LD2CS aluminum alloy test piece typical corrosion pits were observed in this paper every equivalent corrosion year in the experiment accelerated corrosion environment. The box-counting fractal dimension method was employed to extract fractal features of pit outlines, and the evolution rules of typical pit outline fractal dimension values were analyzed. The complexities of the inner and surface corrosion pit morphology were quantitatively analyzed. The conclusions were listed below.

(1) When the scale δ was smaller or larger, the standard deviation was rather large. In order to assure the data validity, fractal dimension data were gathered statistically only when δ was in the interval from 2^3 to 2^7, and the standard deviation threshold was 0. 200.

(2) The surface pit outline fractal dimension reached the maximum in the middle of the corrosion period and became smaller in the earlier or later period. In the later period, surface pits tended to be smoother and tendency to be long oval.

(3) During the later period, Corrosion pits started to generate stepped appearances inside surface pits. While analyzing the inner pit outline fractal dimension, it was found that the deeper the pit located, the more complicated the outline would be.

References

[1] Mahendra boopathi, M. , K. P. Arulshri, et al. Evaluation of mechanical properties of aluminium alloy2024 reinforced with silicon carbide and fly ash hybrid metal matrix composites[J]. American Journal of Applied Science, 2013, 10(3): 219-229.

[2] Timothy P. Gabb, Jack Telesman, Brian Hazel, Daviad P. Mourer. The effects of hot corrosion pits on the fatigue resistance of a disk superalloy[J]. Journal of Materials Engineering and Performance, 2010, 19(1): 77-89.

[3] Adeyemi Dayo Isadare, Bolaji Aremo, Mosobalgje Oyebamiji adeoye, et al. Effect of heat treatment on some mechanical properties of 7075 aluminium alloy[J]. Materials Research, 2012, 12(3): 125-128.

[4] Marinalda C. Pereira, José W. J. Silva, Heloisa A. Acciari, et al. Morphology characterization and kinetics evaluation of pitting corrosion of commercially pure aluminium by digital image analysis[J]. Materials Sciences and Applications, 2012, 5(3), 287-293.

[5] J. Garzón R, C. Barrero, K. E. García, et al. Morphological analysis and classification of types of surface corrosion damage by digital image processing[J]. Revista Colombiana De Fisica, 2006,38(2): 557-560.

[6] Wei Zhao, YongFang Huang, XuBin Ye, et al. Correlation between the geometric parameters of corrosion pit and stress concentration factor[J]. Applied Mechanics and Materials, 2013, 327: 156-160.

[7] A. Valor, F. Caleyo b, L. Alfonso, et al. Stochastic modeling of pitting corrosion: A new model for initiation and growth of multiple corrosion pits[J]. Corrosion Science, 2007, 49: 559-579.

[8] Zhi Lia, Lijie Chen. Feature recognition of corrosion pit for pre-corroded AA 2524 and statistical analysis[J]. Advanced Materials Research, 2014, 906: 206-267.

[9] ZHANG Youhong, LV Guozhi, CHENG Yueliang, et al. Morphological study on corrosion

damage of aluminum alloy[J]. Corrosion Science and Protection Technology, 2007, 19(4): 272-274.
[10] XING Wei, MU Zhitao, ZHOU Lijian. Research on influence on fatigue life attenuation-based corrosion damage characterization factors[J]. Equipment Environmental Engineering, 2011, 8: 49-58.
[11] CHEN Dinghai, MU Zhitao, SU Weiguo, et al. Extracting fractal characteristics from corrosion morphology of aluminum alloys[J]. Journal of Mechanical Strength, 2012, 34(2): 278-281.
[12] XU Fuqiang, LIU Xiangguo. Variables Screening Methods based on the optimization of RBF neural network[J]. Computer Systems & Applications, 2012, 21(3): 206-208.
[13] Dong Dengke, Wang Junyang. Equivelent environment spectrum research on service calendar time for fighter aircraft[J]. Acta Aeronautica et Astronautica Sinica, 1998, 19(4): 451-455.
[14] MU Zhitao,LIU Wenlin,YU Zhanqiao. Research on accelerated corrosion equivalent conversion method of aircraft service environment[J]. Journal of Naval Aeronautical Engineering Institute, 2007, 22(3): 301-304.
[15] CHEN Qunzhi,SUN Zuodong,HAN Enhou, et al. Study on accelerated corrosion test methods of typical aircraft structure[J]. Equipment Environmental Engineering, 2004, 2(1): 13-17.